IEEE Access
Multidisciplinary | Rapid Review | Open Access Journal

Received June 30, 2017, accepted July 26, 2017, date of publication August 3, 2017, date of current version August 22, 2017.

Digital Object Identifier 10.1109/ACCESS.2017.2734328

Performance Analysis of Novel Bridge Type Dual Input DC-DC Converters

SIVAPRASAD ATHIKKAL, (Student Member, IEEE), GANGAVARAPU GURU KUMAR, KUMARAVEL SUNDARAMOORTHY, (Senior Member, IEEE), AND ASHOK SANKAR, (Senior Member, IEEE)

Department of Electrical Engineering, National Institute of Technology Calicut, Kozhikode 673 601, India

Corresponding author: Sivaprasad Athikkal (sivanuday@gmail.com)

ABSTRACT In this paper, two novel bridge type dual input dc–dc converter topologies are introduced for integrating two input energy sources. Out of the two topologies, the latter topology is an improved version of the former one. Both converters have the capability to simultaneously deliver power to the load from the input energy sources. The major advantages of the improved converter as compared with the basic topology are its capability to perform the buck, boost, and buck–boost modes of operation using the same structure and the ability to deliver power to the load even with the failure of any one of the input energy sources. Hence, the detailed software simulation of the improved converter has been performed using MATLAB/Simulink platform. Different analyses have been conducted by considering the parameters, such as the equivalent series resistance of the passive elements in the converter and efficiency of the converter, for better validation of the converter performance. The hardware prototype of the improved converter has been developed in the laboratory environment and tested successfully. The proposed converters have certain merits like less component count, compact structure, and efficient energy utilization, compared with existing converter topologies, which are already reported in the literature.

INDEX TERMS Dual input bridge type dc-dc converters, hybrid energy system, multi-input dc-dc converters, non-conventional energy sources.

NOMENCLATURE

V_1, V_2	Source voltage 1, source voltage 2
V_L, I_L	Inductor voltage and current
I_1, I_2, I_3	Average values of source currents
d_1, d_2, d_3	Duty ratios of switches S_1, S_2 and S_3
d_m	Duty ratio of the mode selection switch
V_0, I_0	Converter output voltage and current
V_{in}	Average value of input source voltages
r_{L_esr}	Equivalent series resistance of the inductor
r_{C_esr}	Equivalent series resistance of the capacitor
L	Inductance
T, f_s	Time period and switching frequency
R	Load Resistance

I. INTRODUCTION

The hybrid energy system is a highly promising technology which can accommodate different non-conventional energy sources to meet varying rural and urban electricity needs. The concept of Hybrid Energy System (HES) is incomplete without a proper power electronic interface [1], [2]. Conventionally, extensive use of parallel coupled single input DC-DC converters has been promoted to integrate multiple numbers of input sources. But, high system complexity, high cost, lower efficiency and dropping of compactness of the system are significant drawbacks of this method. The concept of Multiple Input DC-DC Converter (MIC) has been developed to nullify these demerits. Comparatively simple and compact structure, lower part counts, and higher efficiency are the potential merits of multiple input DC-DC converters (MICs) [3]–[5].

The isolated and non-isolated types of MIC are widely reported in the literature. In isolated topologies, the presence of multi-winding transformers provides electrical isolation but increases the system complexity and cost compared to non-isolated topologies. A flux additivity based MIC is proposed in [6]. Here, the sources are integrated in the magnetic form rather than electrical form. Hence the use of non-isolated MIC is favored in the applications where efficiency and cost of the system are significant concerns. A generalized approach for the development of MICs is illustrated in [7]–[9]. A MIC which is working on buck-boost operation

is presented in [10]. A new MIC for solar – PV and fuel cell applications is proposed in [11]. A non-isolated MIC with bidirectional power flow capability for electric vehicle application is presented in [12]. The converter is well suited for the power management of hybrid energy storage systems. In [13] a dual input DC-DC converter is introduced for high/low voltage sources integration. A MIC for the bidirectional interfacing of DC voltage source is proposed in [14]. But the lower system efficiency due to the power losses associated with the reverse recovery currents of the output diodes is a major demerit of the converter.

A non-isolated MIC for solar-PV application is described in [15]. But the drawback of the converter is that it delivers power from one energy source at a time, and simultaneous power delivery from the input sources are not possible. The concept of a multiport DC-DC converter with a combination of DC-link and magnetic coupling is presented in [16]. A high step-up DC-DC converter and a multiple input voltage summation converter are reported in [17] and [18]. For *n*-input mode, the above converters require '*n*' number of switches and inductors due to which the system becomes complex and expensive. The idea of MICs to manage the power flow from the input supply sources for electric vehicle application is discussed in [19]–[21]. A bidirectional MIC for fuel cell/EV application was developed in [22]. But due to the discontinuous input current, this converter is unsuitable for solar-PV or other renewable energy applications. An extendable multi input step-up DC-DC converter for the efficient integration of non-conventional energy sources is proposed in [23]. Even though the converter has higher voltage gain, the converter has n-inductors and capacitors, and 2n-1 number of diodes for the n-input condition, which increases the complexity of the system and reduces the compactness of the converter.

So, a large number of DC-DC converters are reported in the literature. The converters reported in the literature can be effectively used for hybridization of different energy sources for various applications. Some of them have limitations for simultaneous power delivery from the input energy sources; while others require sophisticated control strategies even though they are capable of individual and simultaneous power supply. Certain MICs have only unidirectional power flow capability which limits their use in applications like electric vehicle where bidirectional power flow capability is mandatory. In this paper, two dual input DC-DC converters are presented in which one converter is the improved form of the other converter. The efficiency of DC-DC converter heavily relies on the total number of components present in the converter. The converters introduced in this paper have higher efficiency compared to other MICs reported in the literature due to its simple and compact structure. Here the proposed topologies can be named as Bridge type Dual Input DC-DC (BDC) Converter and Improved Bridge type Dual Input DC-DC (IBDC) converter. Actually, IBDC converter is derived from BDC converter. The principle of operation and working modes of both converters are discussed in the following sections. The proposed IBDC converter is capable of performing the basic operations of a DC-DC converter such as buck, boost and buck-boost. This converter is also capable of supplying power from the input sources individually and simultaneously. Detailed study of the IBDC converter has been carried out for validating the converter performance.

II. DUAL INPUT DC-DC CONVERTERS

In this section, the detailed description of both BDC and IBDC converters are illustrated. Initially, the analysis of BDC converter is explained with necessary circuit diagrams followed by the detailed working description of IBDC converter.

A. BRIDGE TYPE DUAL INPUT DC-DC (BDC) CONVERTER

The converters mentioned in many of the literature are capable of only the individual power delivery from the connected energy sources to the load. Hence a novel DC-DC converter is introduced in [24] which is proficient in supplying power to the load either individually or simultaneously. The circuit representation of BDC converter is shown in Fig. 1. Here, two input energy sources, i.e., V_1 and V_2 are considered for the analysis of the BDC converter. The power flow between the input sources and the load is managed by adjusting the duty ratios of power switches (S_1, S_2 and S_3) available in the converter. The analytical waveforms of both BDC and IBDC converters in steady state condition are given in Fig. 2. Four Operating states of the BDC converter based on the analytical waveforms are shown in Fig. 3(a-d).

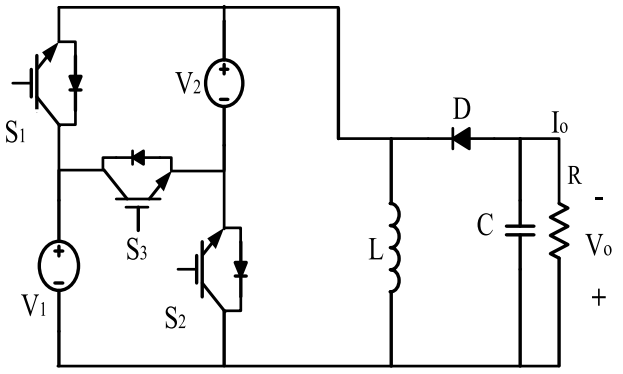

FIGURE 1. Circuit representation of BDC converter.

Operating State-1: In this state, the switch S_1 is turned ON, while the switches S_2, S_3 and diode D are turned OFF. So the source V_1 charges the inductor as shown in Fig. 3(a).

Operating State-2: Here, the switch S_2 is turned ON, while the switch S_1, S_3 and diode D are turned OFF. Thus the source V_2 charges the inductor as shown in Fig. 3(b).

Operating State-3: In this state, only the switch S_3 is operating as shown in Fig. 3(c) which helps to make a series connection of input energy sources together. Therefore, in this operating state, the inductor is charged by the simultaneous contribution from both voltage sources. This is one of the potential merits of the proposed converter in which the

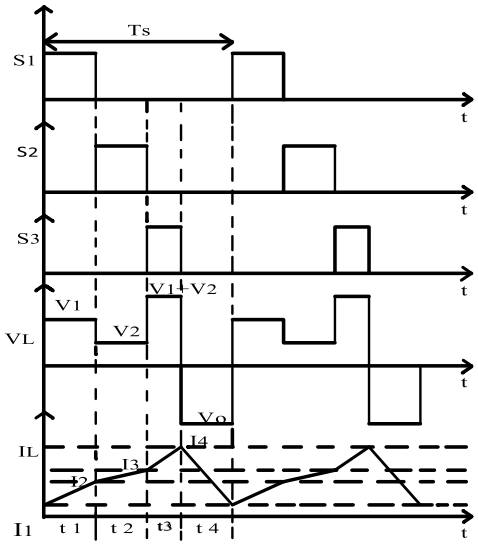

FIGURE 2. Analytical waveforms of switching signal, inductor voltage and current, for BDC and IBDC converters.

individual and simultaneous utilization of both input sources are possible [24].

Operating State-4: In this state, switches S_1, S_2, and S_3 are turned OFF. Thus the stored energy in the inductor simultaneously charges the capacitor and supplies the load through the diode D which is forward biased as shown in Fig. 3(d).

Even though the proposed BDC converter has the merit of supplying the connected energy sources individually and simultaneously, it operates only in the buck-boost type of operation which can be easily noticed from the circuit shown in Fig. 1 which pulls down the significance of the converter in a wide variety of applications. To overcome this problem, the proposed BDC converter has been modified by adding an extra power switch and diode to make it possible to perform all the possible operations of the DC-DC converter such as buck, boost and buck-boost modes. Since the converter is an improved form of the BDC converter, it can be named as Improved Bridge type DC-DC (IBDC) converter.

B. IMPROVED BRIDGE TYPE DUAL INPUT DC-DC (IBDC) CONVERTER

The basic circuit representation of IBDC converter is shown in Fig. 4. The IBDC converter contains four power switches (S_1, S_2, S_3 and S_m) and two diodes (D_1 and D_2). If the IBDC converter needs to operate in the bidirectional mode, the diodes must be replaced by the power switches with an anti-parallel diode. By doing this, it is possible to operate the IBDC converter in the bidirectional mode which is an essential feature for the electric vehicular application, wind energy conversion system, etc. The individual and simultaneous operation of the input energy sources of the converter is accomplished by controlling the power switches S_1, S_2, and S_3. The possible operating modes of the IBDC converter (boost, buck-boost and buck) are decided by the conduction of the power switch S_m, and the two diodes available in the converter. The IBDC converter has four operating

TABLE 1. Possible operating states of IBDC converter in buck-boost operation.

Operating state	Sources supplying	Operating switch	Inductor voltage	Inductor status
State-1	V_1	S_1, S_m	V_1	Charging
State-2	V_2	S_2, S_m	V_2	Charging
State-3	V_1+V_2	S_3, S_m	V_1+V_2	Charging
State-4	None	D_1, D_2	- V_0	Discharging

states in buck-boost operation as shown in Fig.5(a-d), and the details are briefly mentioned in Table 1. The operating states of the IBDC converter in buck-boost operation are same as the operating states of the BDC converter as mentioned earlier. For the simple representation of the circuits in different operating states, the power switches in Fig. 4 have been represented as SPST switches in all the three modes of operation.

C. BUCK AND BOOST OPERATION OF IBDC CONVERTER

The proposed IBDC converter is capable of buck and boost operations also. These operations can be achieved by a proper control of different semiconductor switches available in the IBDC converter. The converter operating states under buck operation is illustrated in Fig. 6(a-d).

State 1: During state 1, the switch S_1 and diode D_2 are in conduction, while all other switches are non-conducting. So, the inductor is charged by the source V_1 as shown in Fig. 6(a).

State 2: Here only the switch S_2 and diode D_2 are in conduction. So, the source V_2 charges the inductor as shown in Fig. 6(b).

State 3: In this state, the inductor is charged by both the input sources ($V_1 + V_2$), which are connected in series. The power switch $S_3$is in conduction to make the input sources in series as given Fig. 6(c).

State 4: This state is similar to that of the freewheeling state of buck-boost operation of the converter. Here, the stored energy in the inductor is delivered to the load through diodes D_1 and D_2.

Boost Operation: The operating states (state 1 and state 2) of the converter in boost operation are depicted in Fig. 7(a) and Fig.7(b). From the figures, it can be noticed that these working states are exactly same as the state 1 and state 3 of the converter in buck-boost operation (Fig. 5(a) and Fig. 5(c)), which is already described. The third working state of the converter in boost operation is shown in Fig. 7(c). In this state, switch S_2 is turned ON while the switches S_1, S_3 and S_m are turned OFF. Hence in this state, the inductor is charged by the source V_2 and simultaneously supplies power to the load.

D. ANALYSIS OF THE IBDC CONVERTER

The analysis of the IBDC converter in Continuous Conduction Mode (CCM) has been carried out in buck-boost operation under steady state condition. The inductor voltage

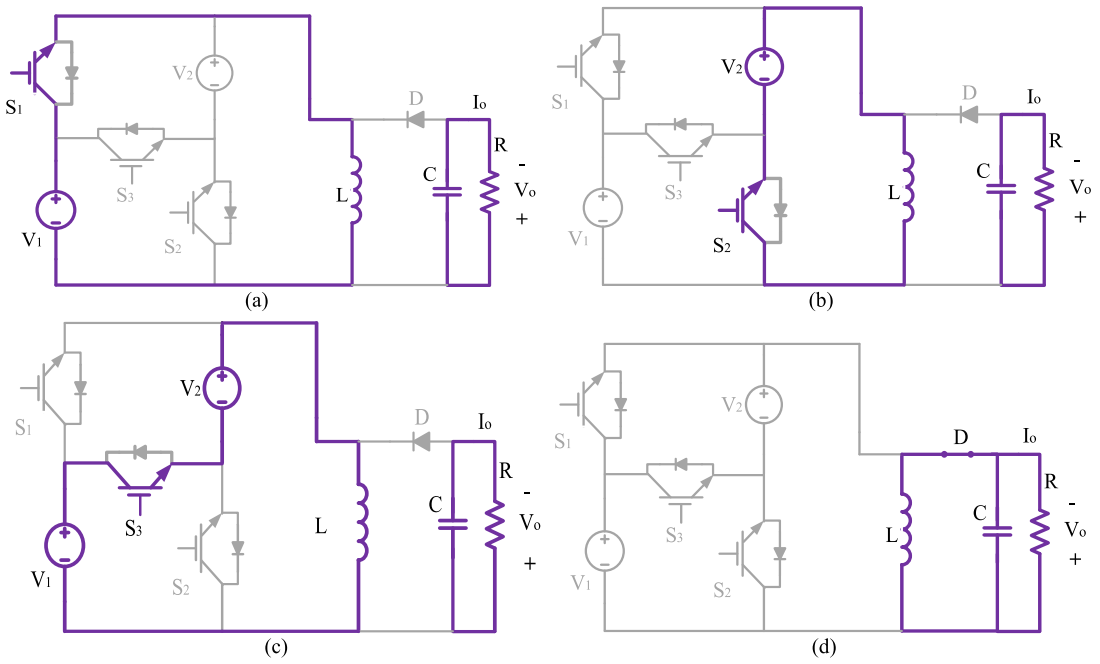

FIGURE 3. Different operating states of the BDC converter. (a) Source V_1 charges the inductor. (b) Source V_2 charges the inductor. (c) Sources V_1 and V_2 together charge the inductor. (d) Freewheeling period of the load current.

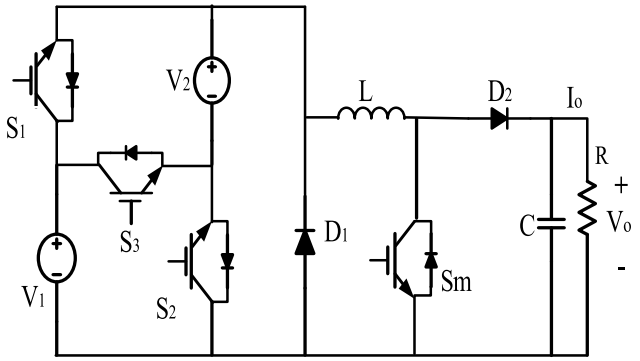

FIGURE 4. The basic circuit of the proposed IBDC converter.

and current variations of the converter are already shown in Fig. 2 for the change of operating states over a single switching cycle. The necessary analytical equations of the IBDC converter under four different working states which are already discussed at the beginning of this section are given below.

State 1: In this state, the inductor voltage is V_1. Since the inductor voltage is a positive value (i.e., $V_1 \geq 0$), the current through the inductor linearly rises from the initial value (i.e., $I_{L(0)}$). So the value of inductor current is obtained as given in (1).

$$I_L = I_{L(0)} + \frac{1}{L}\int_0^{d_1 T} V_L \, dt \tag{1}$$

Here, $V_L = V_1$, hence (1) becomes

$$I_L = I_{L(0)} + \frac{1}{L}(V_1)d_1 T \tag{2}$$

State 2: In this state, the voltage across the inductor is V_2. Here it is considered that $V_1 \geq V_2$, hence the slope of the inductor current is smaller than the preceding interval. So, the inductor current during this interval is given in (3).

$$I_L = I_{L(1)} + \frac{1}{L}\int_{d_1 T}^{(d_1+d_2)T} V_L \, dt \tag{3}$$

In this state, $V_L = V_2$, hence (3) becomes

$$I_L = I_{L(1)} + \frac{1}{L}(V_2)d_2 T \tag{4}$$

State 3: In this state, the voltage across the inductor is $V_1 + V_2$. Since the inductor voltage in this state is higher compared to the previous states, the inductor current slope is larger than the last interval. The value of inductor current during this state is given in (5).

$$I_L = I_{L(2)} + \frac{1}{L}\int_{(d_1+d_2)T}^{(d_1+d_2+d_3)T} V_L \, dt \tag{5}$$

Since, $V_L = V_1 + V_2$, (5) becomes

$$I_L = I_{L(2)} + \frac{1}{L}(V_1 + V_2)d_3 T \tag{6}$$

State 4: In this state, the energy stored in the inductor is delivered to the load through diodes D_1 and D_2. So, the inductor current can be derived as:

$$I_L = I_{L(3)} + \frac{1}{L}\int_{(d_1+d_2+d_3)T}^{T} V_L \, dt \tag{7}$$

In this case, $V_L = -V_o$; So, (7) becomes

$$I_L = I_{L(3)} - \frac{1}{L}V_o\left[T\,(1-(d_1+d_2+d_3)\right] \tag{8}$$

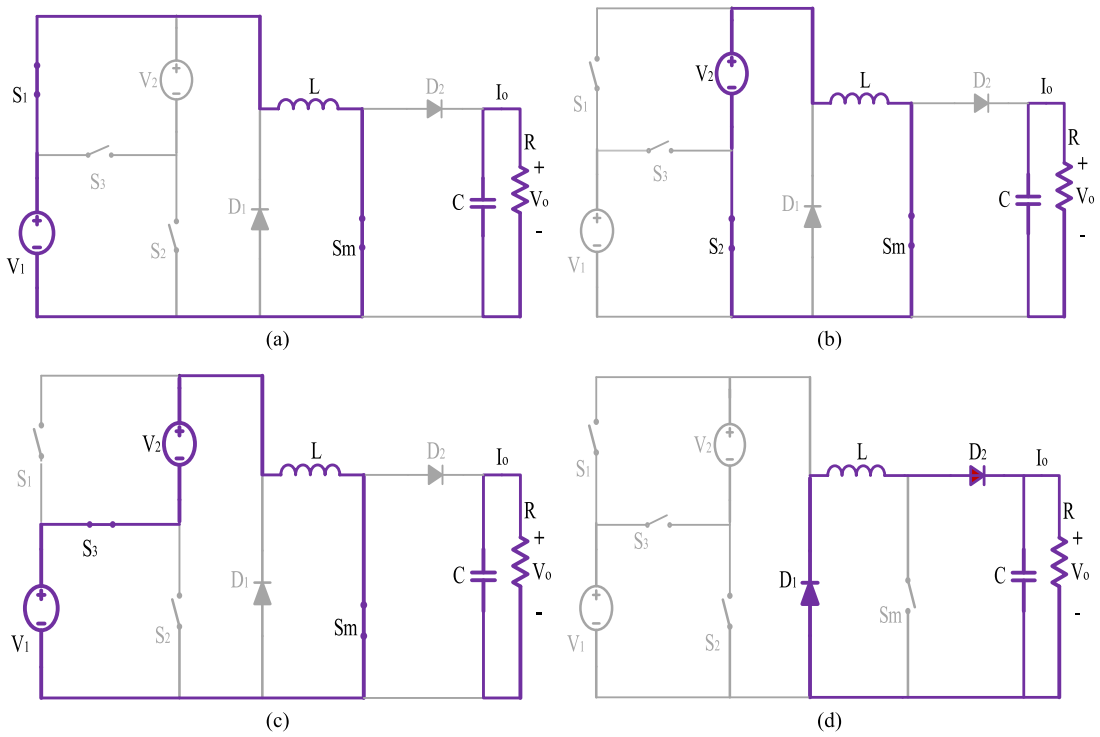

FIGURE 5. Different operating states of IBDC converter during buck-boost operation. (a) Contribution from source 1. (b) Contribution from source 2. (c) Contribution from both sources V_1 and V_2 together. (d) Freewheeling period.

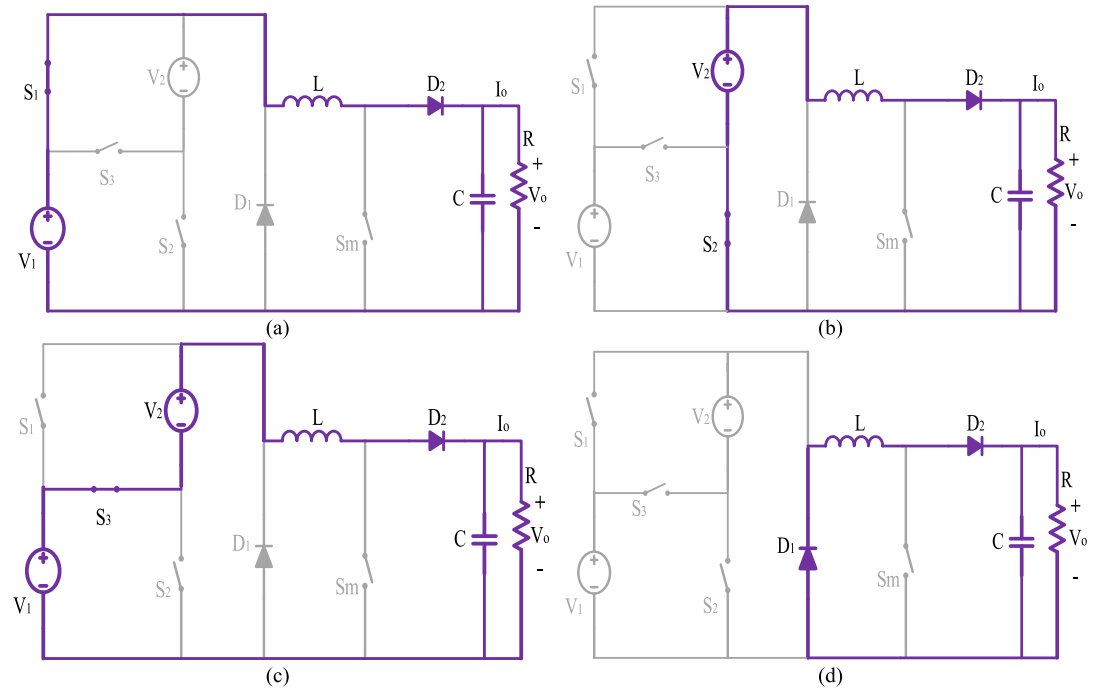

FIGURE 6. Different operating states of IBDC converter during buck operation. (a) Source 1 charges the inductor and supplies the load. (b) Source 2 charges the inductor and supplies the load. (c) Source 1&2 together charge the inductor and supply the load. (d) Freewheeling period.

Here, the inductor voltage is negative, (i.e., $-V_o < 0$) so the inductor current decreases from its previous value ($I_{L(2)}$). As per the volt-second balance equation, the expression for voltage in terms of average values of the input voltage and the output voltage is given as:

$$V_1 d_1 + V_2 d_2 + (V_1 + V_2)\, d_3 - V_0\,(1 - d_1 - d_2 - d_3) = 0 \tag{9}$$

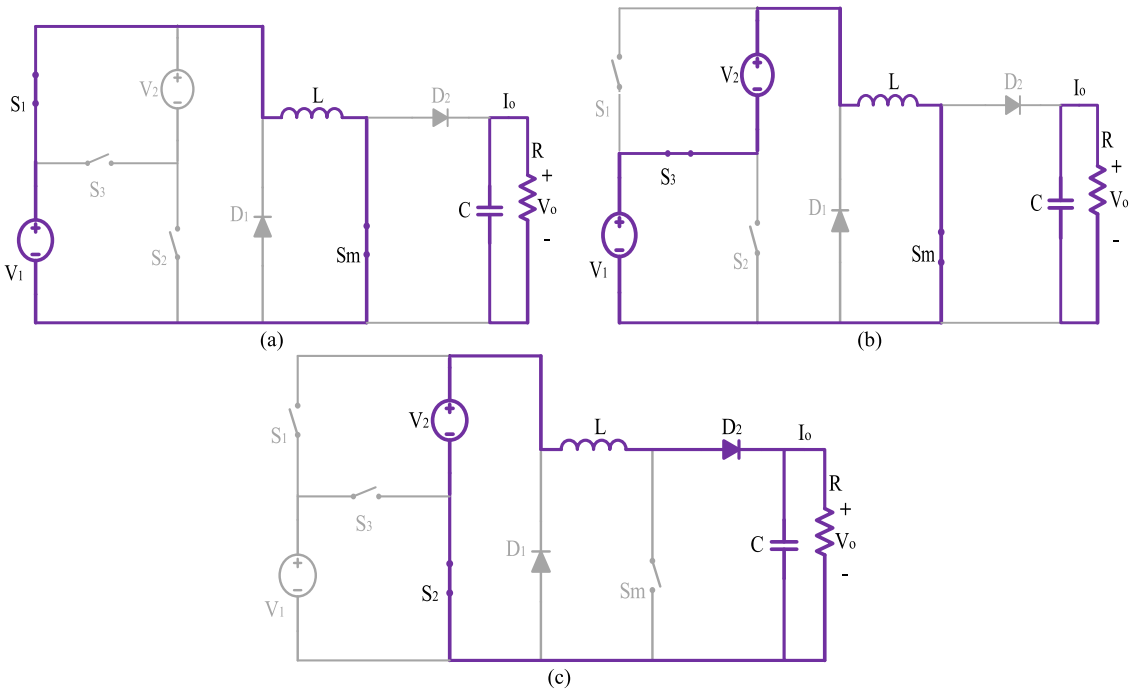

FIGURE 7. Different operating states of IBDC converter during Boost operation. (a) Source 1 charges the inductor. (b) Source 1&2 together charge the inductor. (c) Source 2 charges the inductor and supplies the load.

From the above expression, the output voltage of the converter is given in (10).

$$V_0 = \frac{V_1 d_1 + V_2 d_2 + (V_1 + V_2)\, d_3}{(1 - d_1 - d_2 - d_3)} \tag{10}$$

For a lossless system, it is assumed that the input and output power of the converter are equal as given in (11).

$$V_0 I_0 = V_1 I_1 + V_2 I_2 + (V_1 + V_2)\, I_3 \tag{11}$$

Hence, the output current of the converter is expressed as given in (12).

$$I_0 = \frac{V_1 I_1 + V_2 I_2 + (V_1 + V_2)\, I_3}{V_0} \tag{12}$$

After substituting the value of V_0 from (10) in (12), the expression of I_0 is obtained as:

$$I_0 = \frac{(V_1 I_1 + V_2 I_2 + (V_1 + V_2)\, I_3)(1 - d_1 - d_2 - d_3)}{V_1 d_1 + V_2 d_2 + (V_1 + V_2)\, d_3} \tag{13}$$

Here it is possible to express the average value of source current I_1, I_2 and I_3 in terms of the inductor current, as $I_1 = d_1 I_L$, $I_2 = d_2 I_L$, $I_3 = d_3 I_L$. Hence, by substituting the average values of I_1, I_2 and I_3 in terms of inductor current in (13), the output current is depicted as given below:

$$I_0 = \frac{(V_1 d_1 + V_2 d_2 + (V_1 + V_2)\, d_3)\,(1 - d_1 - d_2 - d_3)\, I_L}{V_1 d_1 + V_2 d_2 + (V_1 + V_2)\, d_3} \tag{14}$$

Finally, the expression for I_0 after simplifying (14) is given as:

$$I_0 = (1 - d_1 - d_2 - d_3)\, I_L \tag{15}$$

From (15), the expression for inductor current I_L is obtained as:

$$I_L = \frac{I_0}{(1 - d_1 - d_2 - d_3)} \tag{16}$$

After substituting the value of I_L from (16), the value source currents I_1, I_2 and I_3 is derived as $I_1 = \frac{d_1 I_0}{(1-d_1-d_2-d_3)}$, $I_2 = \frac{d_2 I_0}{(1-d_1-d_2-d_3)}$, $I_3 = \frac{d_3 I_0}{(1-d_1-d_2-d_3)}$

Finally, the relation between the source currents with respect to duty ratios is depicted as:

$$\frac{I_1}{I_2} = \frac{d_1}{d_2}, \quad \frac{I_2}{I_3} = \frac{d_2}{d_3}, \quad \frac{I_1}{I_3} = \frac{d_1}{d_3} \tag{17}$$

From (17), it is clear that the average source current can be varied by adjusting the duty ratios of the corresponding switches.

The mode selection switch S_m is in ON condition during the period $[(d_1 + d_2 + d_3)T]$ in the buck-boost operation of the converter. Hence the duty ratio of S_m is taken as d_m where it is equal to $(d_1 + d_2 + d_3)$. So the volt-second balance expression given in (9) is generalized as given in (18).

$$V_{in} d_m - V_0 (1 - d_m) = 0 \tag{18}$$

Where, V_{in} is the average value of input voltage sources. So the general expression for the voltage gain of the proposed

TABLE 2. Description of the IBDC converter in all the Possible Working types.

Mode	Input Voltage		Duty Ratio			Output Voltage	Switches (ON)	Switches (OFF)
buck	V_1	V_2	d_1	d_2	d_3	$v_0 = v_1d_1 + v_2d_2 + (v_2 + v_2)d_3$	S_1,S_2,S_3	D_1,D_2
buck-boost	V_1	V_2	d_1	d_2	d_3	$v_0=\frac{v_1d_1+v_2d_2+(v_1+v_2)d_3}{(1-d_1-d_2-d_3)}$	S_1,S_2,S_3,S_m	D_1,D_2
boost	V_1	V_2	d_1	d_2	d_3	$v_0 = \frac{v_1(d_1+d_3)+v_2(1-d_1)}{(1-d_1-d_3)}$	S_1,S_2,S_3,S_m	S_2, D_2

IBDC converter is given as:

$$\frac{V_0}{V_{in}} = \frac{d_m}{(1-d_m)} \tag{19}$$

The brief description of buck, buck-boost and boost operation of the IBDC converter is illustrated in Table 2.

E. EFFECT OF PARASITIC RESISTANCE OF THE PASSIVE ELEMENTS IN THE VOLTAGE GAIN OF THE IBDC CONVERTER

The inductor and capacitor available in the DC-DC converter are not ideal components with only inductance and capacitance. Hence in the practical system, a series resistance is added with the inductor and capacitor to treat them as ideal components. This resistance can be termed as ''Equivalent Series Resistance (ESR)'' of the inductor and capacitor. Various analyses of the proposed IBDC converter are carried out by considering the ESR of the inductor and capacitor available in the converter. The circuit representation of the proposed IBDC converter with the ESR is shown in Fig. 8.

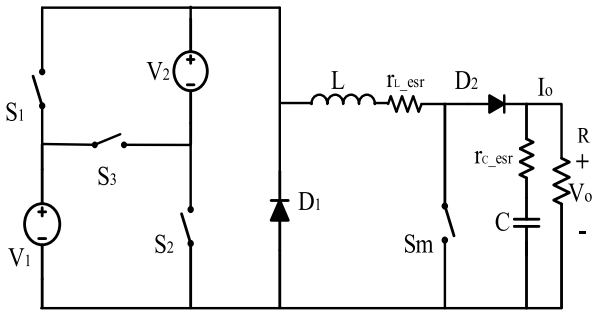

FIGURE 8. Equivalent circuit representation of the proposed IBDC converter with ESR of inductor and capacitor.

1) EFFECT OF INDUCTOR ESR ON THE VOLTAGE GAIN OF THE IBDC CONVERTER

The ESR of the inductor has a significant influence on the voltage gain of the IBDC converter. The inductor voltage of the converter after considering the ESR of the inductor in buck-boost operation is given as follows:

$$\left.\begin{aligned} V_L &= V_1 - I_L r_{L\_esr} \quad for\ d_1 \\ V_L &= V_2 - I_L r_{L\_esr} \quad for\ d_2 \\ V_L &= (V_1 + V_2) - I_L r_{L\_esr} \quad for\ d_3 \\ V_L &= -V_0 - I_L r_{L\_esr} \quad for\ (1 - d_1 - d_2 - d_3) \end{aligned}\right\} \tag{20}$$

Where, r_{L_esr} is the ESR of the inductor.

Hence in a general form, the volt-second balance expression including the inductor ESR is depicted as follows:

$$d_m\left(V_{in} - I_L r_{L\_esr}\right) + (1 - d_m)\left(-V_0 - I_L r_{L\_esr}\right) = 0 \tag{21}$$

After simplification of (21), the expression of the average input voltage of the converter is derived as follows:

$$V_{in} = \frac{V_0\,(1 - d_m) + I_L r_{L\_esr}}{(d_m)} \tag{22}$$

After substituting the value of I_L which is given in (16), in (22), the average input voltage of the converter is derived as follows:

$$V_{in} = \frac{V_0\,(1 - d_m) + \frac{I_0}{(1-d_m)} r_{L\_esr}}{(d_m)} \tag{23}$$

In (16), let $d_1 + d_2 + d_3 = d_m$. But, $I_0 = \frac{V_0}{R}$, so (23) is rewritten as:

$$V_{in} = \frac{V_0\,(1 - d_m) + \frac{1}{(1-d_m)} \frac{V_0}{R} r_{L\_esr}}{(d_m)} \tag{24}$$

The expression of V_{in} is obtained as given below

$$V_{in} = \frac{V_0[(1 - d_m)^2 R + r_{L\_esr}]}{R\,(1 - d_m)\,(d_m)} \tag{25}$$

Finally, from (25) the voltage gain of the IBDC converter by considering the inductor ESR is formulated as follows:

$$\frac{V_0}{V_{in}} = \frac{R\,(1 - d_m)\,(d_m)}{(1 - d_m)^2 R + r_{L\_esr}} \tag{26}$$

Hence by comparing the expressions of the voltage gain in (19) and (26), it can be concluded that the equivalent series resistance of the inductor reduces the voltage gain of the proposed IBDC converter.

2) EFFECT OF CAPACITOR ESR ON THE VOLTAGE GAIN OF THE IBDC CONVERTER

Like inductor ESR, the ESR of the capacitor also has some impact on the voltage gain of the converter. The inductor voltage of the converter after considering the ESR of the capacitor in buck-boost operation is given as follows:

$$\begin{aligned} V_L &= V_{in} \quad for\ d_m \\ V_L &= -V_0 - (I_L - I_0) r_{C\_esr} \quad for\ (1 - d_m) \end{aligned} \tag{27}$$

Where r_{C_esr} is the ESR of the capacitor.

The volt-second balance expression including capacitor ESR is formulated as follows:

$$d_m\,(V_{in}) + (1 - d_m)\,(-V_0 - (I_L - I_0)r_{C\_esr}) = 0 \quad (28)$$

After simplifying the above equation, the value of the average input voltage is given as follows:

$$V_{in} = \frac{(1 - d_m)\,[V_0 + (I_L - I_0)r_{C\_esr}]}{(d_m)} \quad (29)$$

By substituting $I_L = \frac{I_0}{(1-d_m)} = \frac{V_0}{R(1-d_m)}$ in the above equation, the average input voltage is given as follows:

$$V_{in} = \frac{V_0[(1 - d_m)\,R + d_m r_{C\_esr}]}{R\,(d_m)} \quad (30)$$

The voltage gain of the IBDC converter by considering the ESR of the capacitor is derived as follows:

$$\frac{V_0}{V_{in}} = \frac{R\,(d_m)}{(1 - d_m)\,R + d_m r_{C\_esr}} \quad (31)$$

From the expressions of the voltage gain which are given in (19) and (31), it can be observed that the equivalent series resistance of the capacitor reduces the voltage gain of the proposed IBDC converter.

F. CONTROL STRATEGY FOR IBDC CONVERTER

A MIC should be proficient in extracting different amounts of power from the connected input energy sources while maintaining the proper power supply to the load with the regulated output voltage. So, an appropriate control strategy is a requisite for resolving the power management problems in a MIC. The power control strategy is mainly dependent on the type of input energy sources connected where the dynamic and steady state response of the connected sources are different. Hence, a power control algorithm which can consider the steady state and dynamic characteristics of each connected source would be a better choice for MIC.

1) CONTROL STRATEGY BASED ON AVERAGE CURRENT MODE METHOD

In this paper, a simple power control strategy has been designed and its overall block diagram is shown in Fig. 9. The concept of Average Current Mode (ACM) control of typical power electronic converters has been used for the design of the proposed power control strategy. The ACM control includes either load side control or source side control. In load side control, the current through the inductor is directly monitored and controlled to regulate the load voltage; while in source side control, the inductor current is indirectly controlled by monitoring the respective source currents for a given load condition. The dynamic response of the load side control is poor, even though they have fewer sensor requirements. So the source side control is well suited for the effective utilization of the connected energy source with an excellent dynamic response.

Hence in this work, source side control is implemented. Here, the output voltage is sensed and compared with the reference value. The error has been fed back to a voltage controller (VC) which gives the reference current at the output. In the next stage, scaling of the generated reference current signal has been carried out by the scaling factors derived from the input and output power relationship. The scaling factors Z_1, Z_2, and Z_3 are considered for generating individual reference currents and can be varied between 0 to 1 (ie., $Z_1 \in [0, 1], Z_2 \in [0, 1], Z_3 \in [0, 1]$). Here, the generated individual reference currents are then compared with the actual source currents, and the error has been processed by a current controller that generates PWM pulses for IBDC converter. In this work, PI controller is used to realize voltage and current controllers.

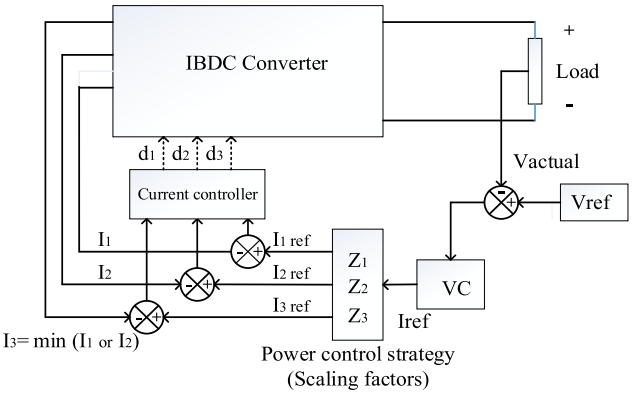

FIGURE 9. Control strategy for IBDC converter based on ACM control.

The gain parameters of these controllers are determined by output voltage to duty ratio and source currents to duty ratio transfer functions obtained from the small signal model of the proposed converter. Here, as the individual reference currents are different for each source current, the power drawn from each source will be different. The variation in particular source current can be clearly indicated by the variation in corresponding scaling factor from 0 to 1. Hence by using this control strategy, it is easy to control the duty ratios of the power switches present in the IBDC converter so that a well-regulated output voltage can be achieved under load side and source side disturbances.

2) CONTROL STRATEGY BASED ON ONE CYCLE CONTROL METHOD

In addition to the above method, a control strategy has been implemented for the proposed IBDC converter with One Cycle Control (OCC) method and the schematic representation of voltage regulating system using OCC shown in Fig. 10 for buck-boost operation. The OCC is helpful for reducing the control complexity by avoiding the control loop interactions. Since it is a nonlinear control strategy, it takes the merits of nonlinear characteristics of power converters and provides instant dynamic control of the switched variable [25], [26]. In this method, the average value of switched variable will reach a new steady state condition within one switching cycle followed by a transient condition. The steady-state or

TABLE 3. Design parameters.

Source 1 (V)	Source 2 (V)	Inductor (mH)	Capacitor (μF)	Switching Frequency (f_s) (kHz)	Output Voltage (V)		
					Buck	Buck-boost	Boost
50	30	7	470	20	20	20/100	100

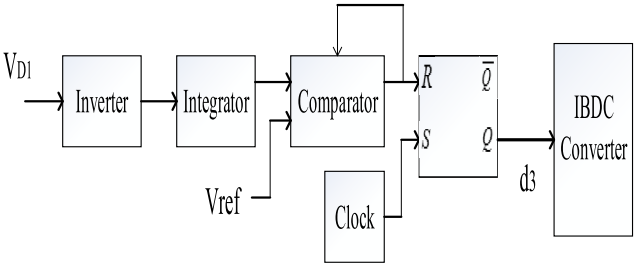

FIGURE 10. Control strategy of IBDC converter with OCC.

dynamic error between the control reference and the average value of the switched variable will be zero in OCC. Hence, OCC is an efficient control method that gives a quick dynamic response, excellent rejection of source side and load side disturbances, robust performance, and instantaneous switching error correction. A multi-input converter under PWM control needs PI controller in voltage control loop and current control loop. These PI controllers should be redesigned till the stability, and satisfactory dynamic responses are achieved. In OCC, there is no requirement of PI controller which significantly reduces the complexity in closed loop design procedures. Here the operation of series switch S_3 alone is considered in OCC for ease of explanation. In this case, two sources supply power to the load simultaneously. So, the average voltage across the diode D_1 is assumed to be equal to the output voltage V_0 by neglecting the drop across the passive elements.

Hence V_{D1} is considered as the control variable for output voltage regulation. Thus the voltage regulating system modulates the duty ratio of the switch S_3 such that the average value of V_{D1} follows the reference voltage in each switching cycle, thereby providing a well-regulated output voltage even if there is a step change in source or step change in load.

As shown in Fig. 10, the voltage regulating system comprises an inverter, a resettable integrator, a comparator, a controller and a clock. The constant frequency clock simultaneously turns on S_3 and activates the integrator at the beginning of each switching period. Thus V_{D1} is integrated and compared with control reference. When the integrated value reaches the control reference *Vref*, the comparator changes its state. As a result, S_3 is turned off, and the integrator is reset to zero until the next clock pulse comes. This ensures fast rejection of load side and source side perturbations which enhance the importance of OCC in MICs.

III. RESULTS AND DISCUSSION

A. SIMULATION RESULTS

The simulation of the IBDC converter is performed using MATLAB/ Simulink platform. The parameters considered for the simulation and experimental purpose of IBDC converter are given in Table 3. The results of IBDC converter obtained from the simulation studies for buck, buck-boost and boost operation are shown in Fig. 11 and Fig. 12. The simulation results for buck operation are illustrated in Fig. 11 (a & b). From the figure, it is evident that the charging voltages of the inductor are 30 V (i.e., V_1-V_O) for duty ratio d_1, 10 V (i.e., V_2-V_O) for duty ratio d_2 and 60 V (i.e., $V_1 + V_2 - V_O$) for duty ratio d_3. Finally, the discharging voltage of inductor is -20 V (i.e., $-V_O$) for the remaining period. Similarly, the performance of the IBDC converter under boost operation is depicted in Fig. 11(c & d). Initially, the inductor is charged by a voltage of 50 V (i.e., V_1) for a duty ratio d_1, and then it is charged by a voltage of 30 V (i.e., V_2) till the switch S_m is turned OFF. Finally, the energy stored in the inductor is delivered to the load with a discharging voltage of -70 V (i.e., V_2-V_O).

The results of the IBDC converter for buck-boost operation are shown in Fig. 12(a-d) for the duty ratio less than 0.5, and greater than 0.5. In both cases, the inductor is charged by a voltage of 50 V (i.e., V_1), 30 V (i.e., V_2) and 80 V (i.e., $V_1 + V_2$) for duty ratios d_1, d_2 and d_3 respectively. Then the stored energy in the inductor is discharged with the voltages of -20V and -100 V for the operation of the IBDC converter with duty ratio (i.e., $d_1 + d_2 + d_3$) less than 0.5 and greater than 0.5 respectively.

B. EXPERIMENTAL RESULTS

The feasibility and performance of the IBDC converter have been verified by developing an experimental prototype in the laboratory environment. Generation of the switching pulses and interfacing with the experimental prototype in real time condition is realized with the help of dSPACE 1104 real time digital controller. The switching frequency of 20 kHz is considered for generating the pulses. In this work, the power switches for IBDC converter are realized by FGH40N120AN IGBT switches, and the diodes are realized by MUR 860 fast recovery diodes. The performance of the converter for all three types of operation such as buck, boost and buck-boost has been verified. The waveforms obtained from the experimentation are shown in Fig. 13 (a-d). The output voltage of the converter is 20 V for buck operation (Fig. 13(a)), and buck-boost operation with duty ratio < 0.5 (Fig. 13(b)). The output voltage is 100 V for buck-boost operation with duty ratio > 0.5 and boost operation also (Fig. 13(c)) and Fig. 13(d)). The experimental waveforms of the IBDC converter when the series switch S_3 is operating as the second switch are shown in Fig. 14 (a-b) for the buck and buck-boost operations. Hence from the analysis, it is noticed that

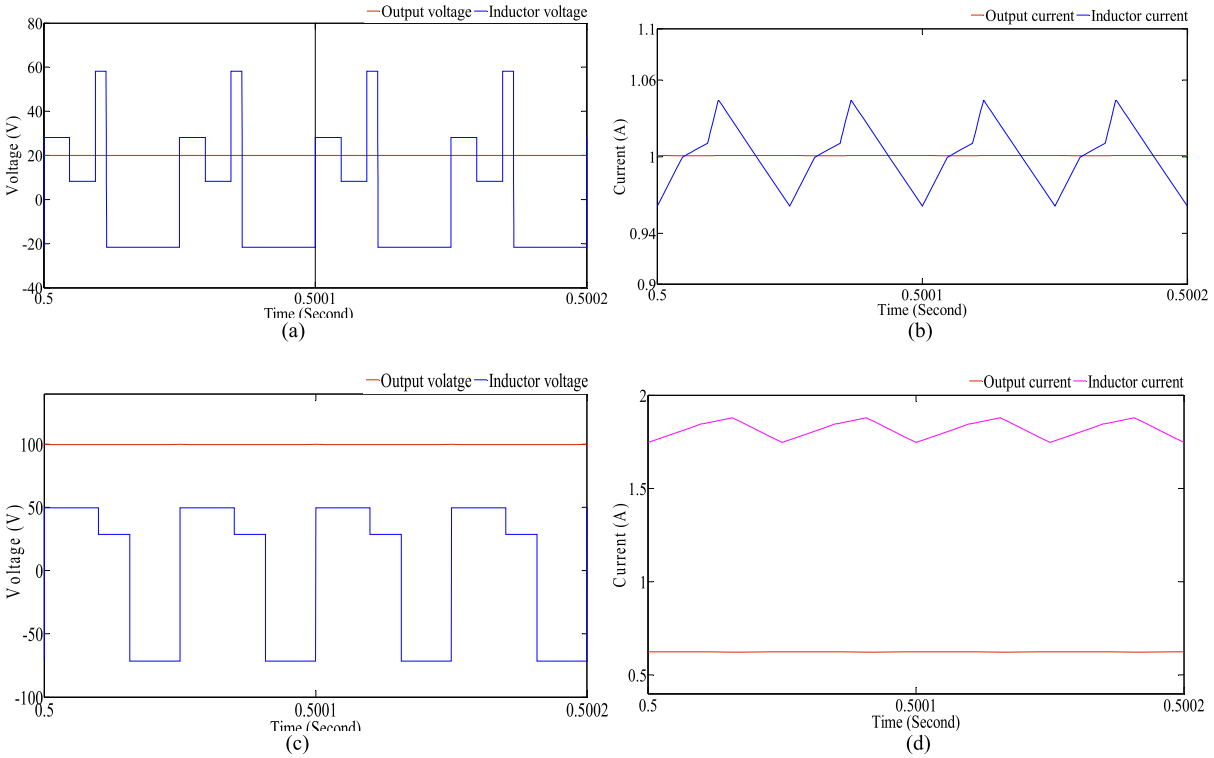

FIGURE 11. Simulation waveforms of IBDC converter (a) Inductor voltage, output voltage (b) inductor current and output current for buck operation (c) Inductor voltage, output voltage (d) inductor current and output current for boost operation.

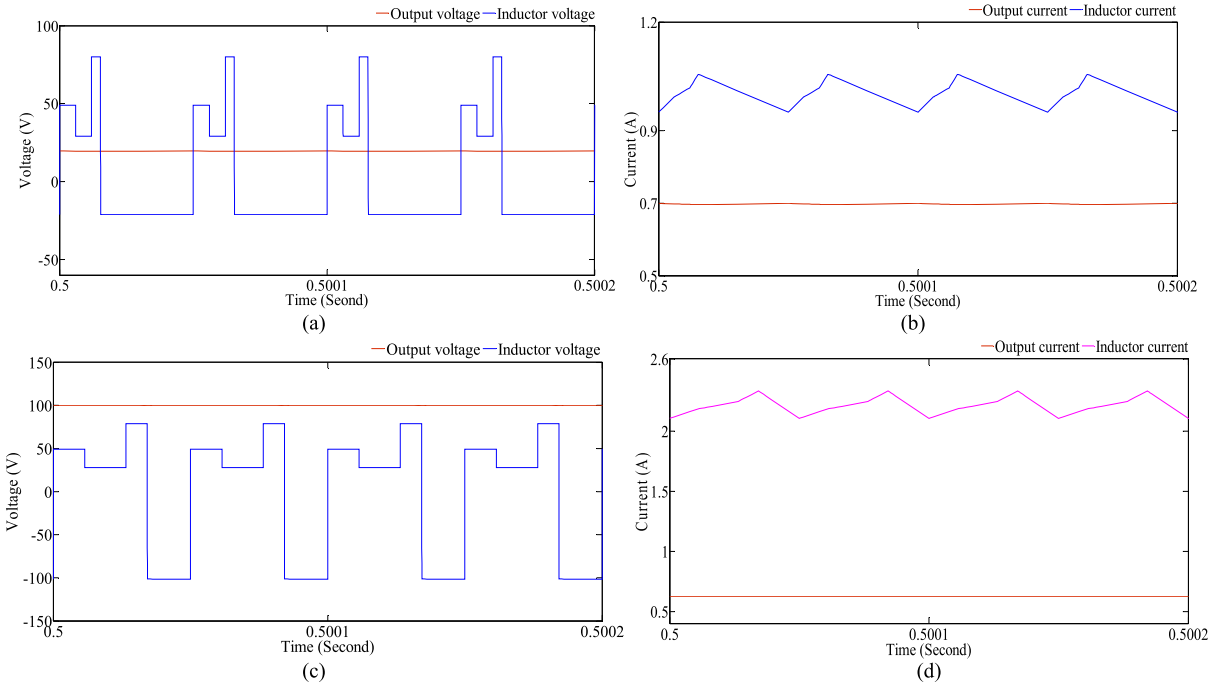

FIGURE 12. Simulation waveforms for buck-boost operation of the IBDC converter (a) Inductor voltage, output voltage (b) inductor current and output current for duty ratio $d_1 + d_2 + d_3 < 0.5$ (c) Inductor voltage, output voltage, (d) inductor current and output current for duty ratio $d_1 + d_2 + d_3 > 0.5$.

the experimental results are well matched with the results obtained from the simulation.

A transient analysis has been carried out to perceive the dynamic behavior of the converter under load and source side perturbations in the buck-boost operation of the IBDC converter using ACM method. The output voltage response due to the load changes is shown in Fig. 15 (a). Here, the output voltage is regulated at the desired value of 100 V

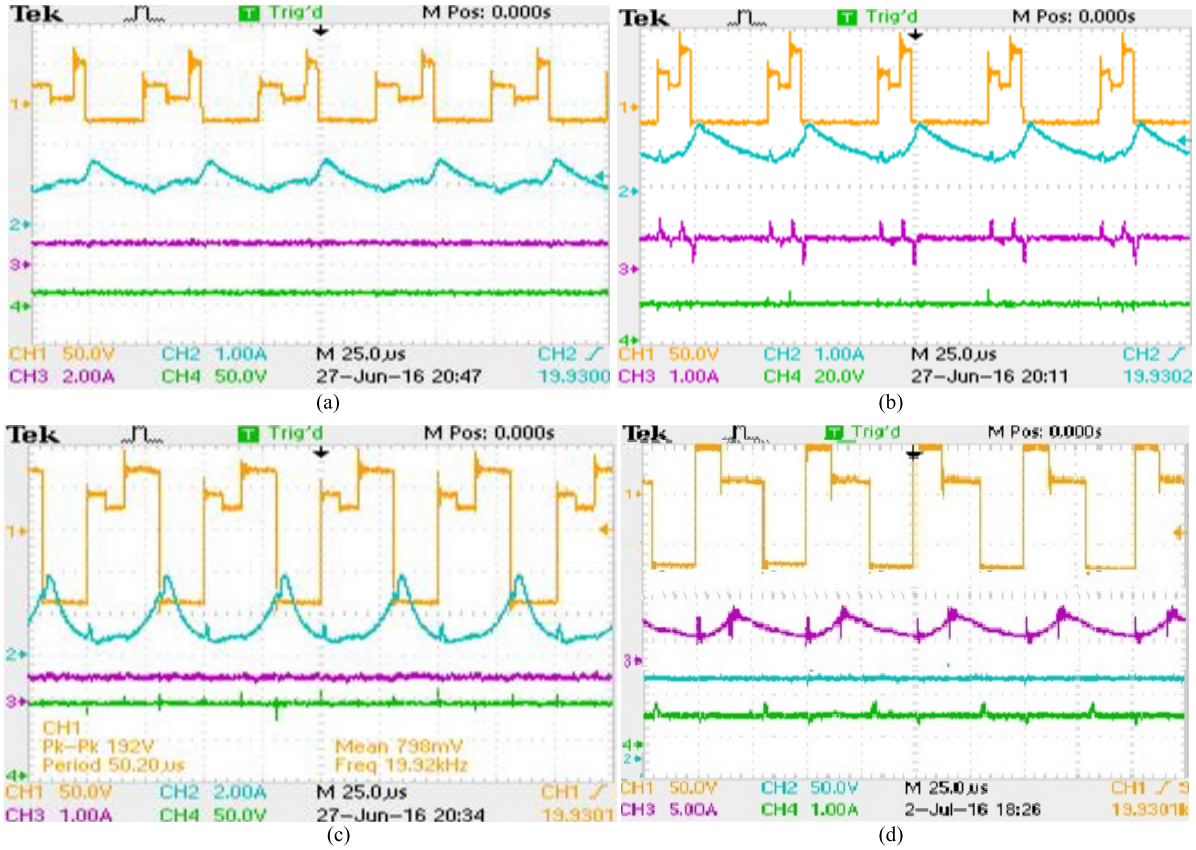

FIGURE 13. Experimental waveforms of the IBDC converter (a) buck (b) buck-boost (duty ratio < 0.5) (c) buck-boost (duty ratio > 0.5) (CH1: inductor voltage, CH2: inductor current, CH3: output current, CH4: Output voltage) (d) Boost (CH1: inductor voltage, CH2: output voltage, CH3: inductor current,CH4: output current) [Switch S_2 operating second] [13 (a) and 13 (c) : CH1 & CH4 =50 V/div, 13(b) : CH1=50 V/div, CH4=20 V/div, 13(d) : CH1&CH2=50 V/div].

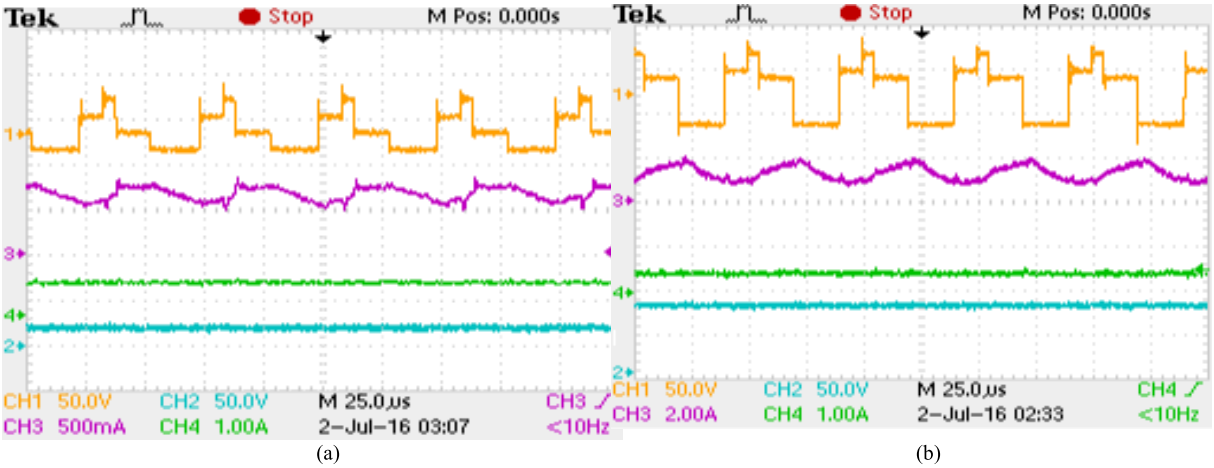

FIGURE 14. Experimental waveforms of inductor voltage, inductor current, output voltage and output current of the proposed converter (a) buck mode of operation (b) buck-boost mode of operation (Series switch S_3 operating second) [CH1&CH2=50 V/div].

under sudden variation of load current from 0.4 A to 1.2 A. Similarly, the output voltage is well regulated at the same value for the step fall of load current from 1.2 A to 0.4 A.

The dynamic behavior of the IBDC converter under varying source conditions is shown in Fig. 15(b). Here, the load is initially supplied by both sources together for a short period. Suddenly, source 1 becomes zero (i.e., a step fall in the source voltage V_1 from 50 V to 0 V) and a small change is observed in the output voltage and load current due to this effect. Similarly, after a short duration the source 1 is back

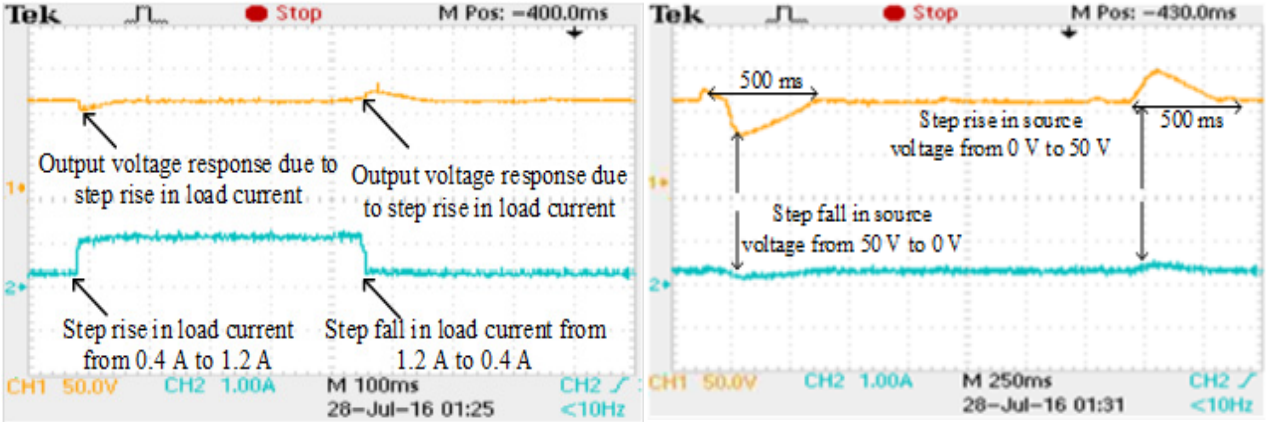

FIGURE 15. Experimental waveforms of the output voltage and load current of the converter (a) under varying load conditions (b) under varying source conditions (CH1: 50 V/div, CH2: 1 A/div) [ACM method].

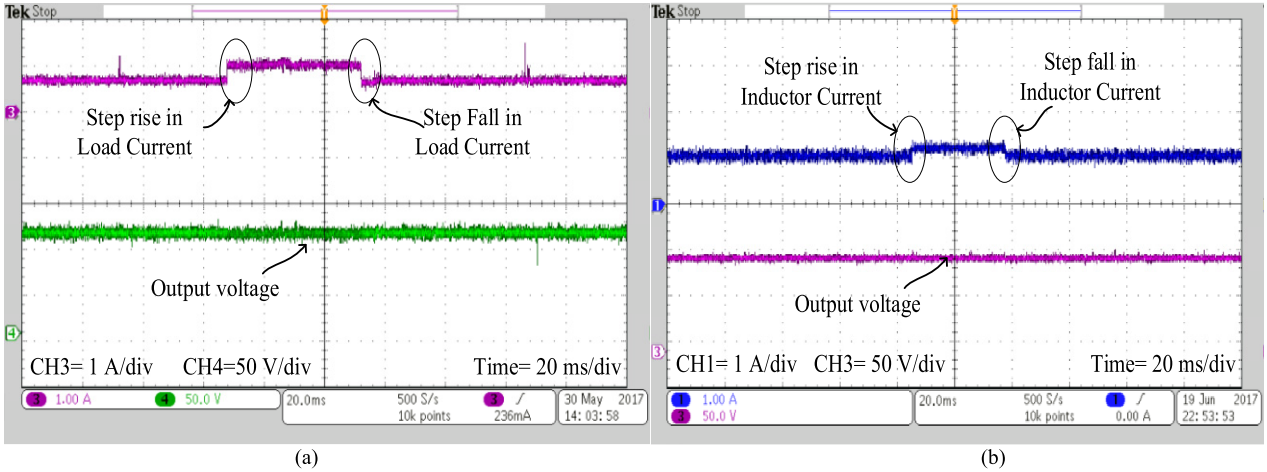

FIGURE 16. Experimental waveforms of the IBDC converter (a) output voltage and load current response due to the load variation (b) output voltage and inductor current response due to the load variations [OCC method].

into the operation (i.e., step rise in V_1 from 0 V to 50 V) and corresponding output voltage and load current response are analyzed. In both the conditions, the output voltage and current maintain their required values even after small variations. The settling time of the converter output voltage for the step variations in source voltage using ACM method is measured and the obtained value is 500 ms which is marked Fig. 15(b). So, from Fig. 15(a) and Fig. 15(b), it can be observed that though there are severe changes in the load current and source voltage values, the output voltage is well regulated at the desired value in a comparatively faster manner.

The experimental waveforms of the converter output voltage and load current response due to the step variations in the load using OCC method are shown in Fig. 16 (a). Similarly, the output voltage and inductor current response due to the sudden load variations are shown in Fig. 16(b). From the figures, it can be clearly observed that the output voltage of the IBDC converter is well regulated at the desired value of 100 V (buck-boost operation with duty ratio>0.5) with a faster dynamic response under sudden load changes compared to the ACM method shown in Fig. 15(a) which shows the efficient operation of the developed OCC in load side perturbation rejection. The experimental waveforms of the output voltage and load current response under step variation in one of the source voltage are shown in Fig. 17(a).

From Fig. 17(a) it is observed that the converter output voltage and load current is well regulated at their desired values without any prominent deviation for the step variations in source voltage. Here in OCC method, the step change in source voltage 2 (i.e., 0 V to 30 V and 30 V to 0) is considered for the transient analysis. In order to verify the dynamic response of the converter under sudden source variations in OCC method, the settling time of the converter output voltage has been calculated, and the obtained value is 4ms for step rise and fall in source voltage which is shown in Fig. 17(b). Hence compared to the settling time of the output voltage using ACM method (i.e., 500ms (Fig. 15(b)) the value

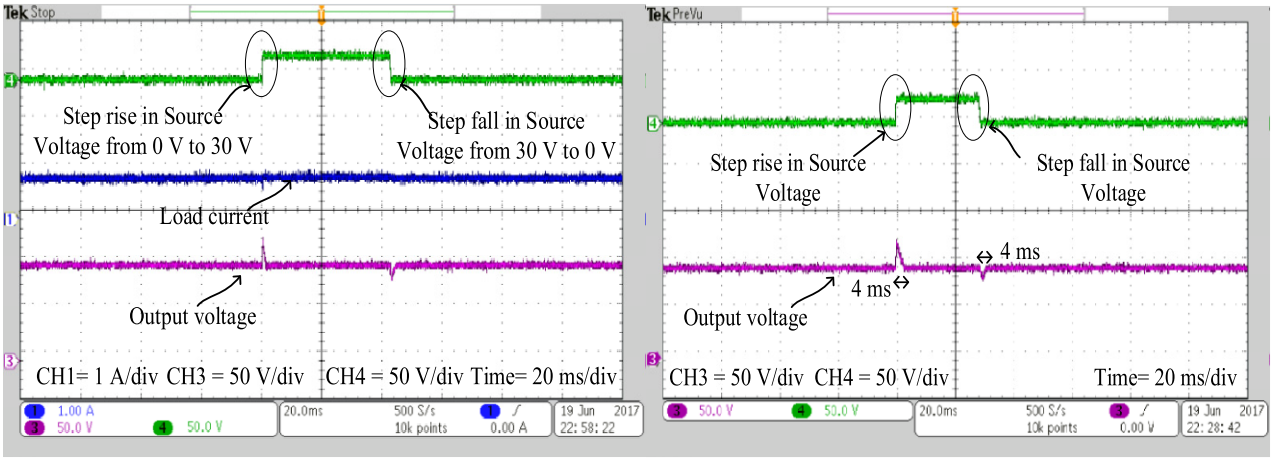

FIGURE 17. Experimental waveforms of the IBDC converter (a) output voltage and load current response due to the source variations (b) output voltage settling time analysis due to the source variations [OCC method].

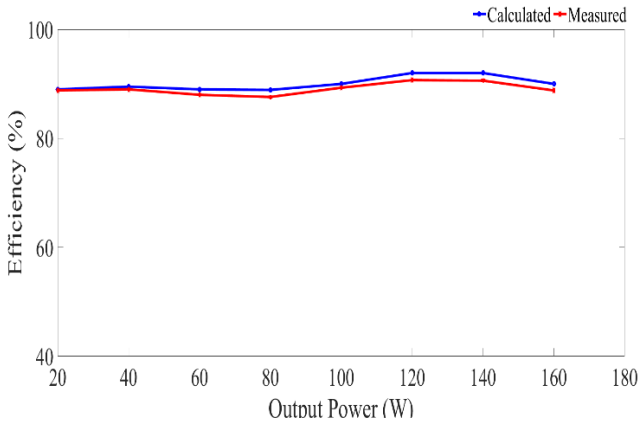

FIGURE 18. Efficiency of the IBDC converter over varied load condition.

of settling time of the output voltage using OCC method (i.e., 4ms) is very small which shows the excellent improvement in the dynamic behavior of the converter using OCC method. Finally, the value of efficiency over varying load condition is depicted in Fig. 18. From the figure, it can be concluded that the proposed IBDC converter has good efficiency profile compared to other topologies which are reported in the literature. The efficiency of the IBDC converter can be improved further by adopting the optimum design of the components available in the converter.

IV. CONCLUSION

Two novel dual input bridge type DC-DC converter (BDC converter and IBDC converter) topologies are proposed in this paper for the integration of hybrid energy sources. Initially, the description and modes of operation of the BDC converter have been presented and then, the detailed analysis of the improved IBDC converter derived from BDC converter has been carried out for three possible modes of operations such as buck, boost an buck-boost. The effect of ESR of the passive elements (capacitor/inductor) in the voltage gain of the converter has been analyzed in a detailed manner. From the ESR analysis, it has been found that the ESR of the inductor and capacitor significantly reduces the voltage gain of the converter . The experimental analysis of the IBDC converter is performed in a comprehensive manner to validate the simulation results. The steady state and dynamic behavior of the IBDC converter are observed using the transient analysis of the converter. Two control strategies (ACM and OCC) have been developed and tested for the regulation of the output voltage at the required value, and the results are compared. From the transient analysis of the IBDC converter in the experimental platform, it is found that OCC method offers excellent dynamic response compared to the ACM method. The BDC and IBDC converters have the compact structure and less component count which enhances their importance in aerospace, microgrid and smart grid applications.

REFERENCES

[1] J. Cao and A. Emadi, "A new battery/ultracapacitor hybrid energy storage system for electric, hybrid, and plug-in hybrid electric vehicles," *IEEE Trans. Power Electron.*, vol. 27, no. 1, pp. 122–132, Jan. 2012.

[2] S. Kumar and H. P. Ikkurti, "Design and control of novel power electronics interface for battery-ultracapacitor hybrid energy storage system," in *Proc. Int. Conf. Sustain. Energy Intell. Syst. (SEISCON)*, Chennai, India, Jul. 2011, pp. 236–241.

[3] A. Khaligh, J. Cao, and Y.-J. Lee, "A multiple-input DC–DC converter topology," *IEEE Trans. Power Electron.*, vol. 24, no. 3, pp. 862–868, Mar. 2009.

[4] W. Jiang and B. Fahimi, "Multiport power electronic interface—Concept, modeling, and design," *IEEE Trans. Power Electron.*, vol. 26, no. 7, pp. 1890–1900, Jul. 2011.

[5] M. A. Rosli, N. Z. Yahaya, and Z. Baharudin, "Multi-input DC–DC converter for hybrid renewable energy generation system," in *Proc. IEEE Conf. Energy Convers. (CENCON)*, Johor Bahru, Malaysia, Oct. 2014, pp. 283–286.

[6] Y.-M. Chen, Y.-C. Liu, and F.-Y. Wu, "Multi-input DC/DC converter based on the multiwinding transformer for renewable energy applications," *IEEE Trans. Ind. Appl.*, vol. 38, no. 4, pp. 1096–1104, Jul./Aug. 2002.

[7] Y.-C. Liu and Y.-M. Chen, "A systematic approach to synthesizing multi-input DC–DC converters," *IEEE Trans. Power Electron.*, vol. 24, no. 1, pp. 116–127, Jan. 2009.

[8] Y. Li, X. Ruan, D. Yang, F. Liu, and C. K. Tse, "Synthesis of multiple-input DC/DC converters," *IEEE Trans. Power Electron.*, vol. 25, no. 9, pp. 2372–2385, Sep. 2010.
[9] A. Kwasinski, "Identification of feasible topologies for multiple-input DC–DC converters," *IEEE Trans. Power Electron.*, vol. 24, no. 3, pp. 856–861, Mar. 2009.
[10] B. G. Dobbs and P. L. Chapman, "A multiple-input DC–DC converter topology," *IEEE Power Electron Lett.*, vol. 1, no. 1, pp. 6–9, Mar. 2003.
[11] E. Babaei and O. Abbasi, "Structure for multi-input multi-output DC–DC boost converter," *IET Power Electron.*, vol. 9, no. 1, pp. 9–19, Jan. 2016.
[12] F. Akar, Y. Tavlasoglu, E. Ugur, B. Vural, and I. Aksoy, "A bidirectional nonisolated multi-input DC–DC converter for hybrid energy storage systems in electric vehicles," *IEEE Trans. Veh. Technol.*, vol. 65, no. 10, pp. 7944–7955, Oct. 2016.
[13] Y. M. Chen, Y. C. Liu, and S. H. Lin, "Double-input PWM DC/DC converter for high-/low-voltage sources," *IEEE Trans. Ind. Electron.*, vol. 53, no. 5, pp. 1538–1545, Oct. 2006.
[14] M. Marchesoni and C. Vacca, "New DC–DC converter for energy storage system interfacing in fuel cell hybrid electric vehicles," *IEEE Trans. Power Electron.*, vol. 22, no. 1, pp. 301–308, Jan. 2007.
[15] M. R. Banaei, H. Ardi, R. Alizadeh, and A. Farakhor, "Non-isolated multi-input–single-output DC/DC converter for photovoltaic power generation systems," *IET Power Electron.*, vol. 7, no. 11, pp. 2806–2816, Nov. 2014.
[16] H. Tao, A. Kotsopoulos, J. L. Duarte, and M. A. M. Hendrix, "Family of multiport bidirectional DC–DC converters," *IEE Proc.-Electr. Power Appl.*, vol. 153, no. 3, pp. 451–458, May 2006.
[17] L. W. Zhou, B. X. Zhu, and Q. M. Luo, "High step-up converter with capacity of multiple input," *IET Power Electron.*, vol. 5, no. 5, pp. 524–531, May 2012.
[18] Y. Yuan-Mao and K. W. E. Cheng, "Multi-input voltage-summation converter based on switched-capacitor," *IET Power Electron.*, vol. 6, no. 9, pp. 1909–1916, Nov. 2013.
[19] Z. Li, O. Onar, A. Khaligh, and E. Schaltz, "Design and control of a multiple input DC/DC converter for battery/ultra-capacitor based electric vehicle power system," in *Proc. 24th Annu. IEEE Appl. Power Electron. Conf. Expo.*, Washington, DC, USA, Feb. 2009, pp. 591–596.
[20] L. Solero, A. Lidozzi, and J. A. Pomilio, "Design of multiple-input power converter for hybrid vehicles," *IEEE Trans. Power Electron.*, vol. 20, no. 5, pp. 1007–1016, Sep. 2005.
[21] A. Di Napoli, F. Crescimbini, S. Rodo, and L. Solero, "Multiple input DC–DC power converter for fuel-cell powered hybrid vehicles," in *Proc. IEEE 33rd Annu. IEEE Power Electron. Spec. Conf.*, Cairns, QLD, Australia, Jun. 2002, pp. 1685–1690.
[22] A. Hintz, U. R. Prasanna, and K. Rajashekara, "Novel modular multiple-input bidirectional DC–DC power converter (MIPC) for HEV/FCV application," *IEEE Trans. Ind. Electron.*, vol. 62, no. 5, pp. 3163–3172, May 2015.
[23] A. Deihimi, M. E. S. Mahmoodieh, and R. Iravani, "A new multi-input step-up DC–DC converter for hybrid energy systems," *Electr. Power Syst. Res.*, vol. 149, pp. 111–124, Aug. 2017.
[24] A. Sivaprasad, G. G. Kumar, S. Kumaravel, and S. Ashok, "A novel bridge type DC–DC converter for hybrid energy source integration," in *Proc. IEEE 1st Int. Conf. Power Electron., Intell. Control Energy Syst. (ICPEICES)*, Delhi, India, Jul. 2016, pp. 1–6.
[25] K. M. Smedley and S. Ćuk, "One-cycle control of switching converters," *IEEE Trans. Power Electron.*, vol. 10, no. 6, pp. 625–633, Nov. 1995.
[26] D. Yang, M. Yang, and X. Ruan, "One-cycle control for a double-input DC/DC converter," *IEEE Trans. Power Electron.*, vol. 27, no. 11, pp. 4646–4655, Nov. 2012.

SIVAPRASAD ATHIKKAL (S'13) was born in Thrissur, India, in 1989. He received the B.Tech. degree in electrical and electronics engineering from University of Calicut, Thenhippalam, India, in 2010, and the M.Tech. degree in power electronics from the Amrita Vishwa Vidyapeetham University, Coimbatore, India, in 2012. He is currently pursuing the Ph.D. degree in electrical engineering with the National Institute of Technology Calicut, India. His main research interests include multiple input dc–dc converters and renewable energy integration.

GANGAVARAPU GURU KUMAR was born in Tenali, India, in 1992. He received the B.Tech. degree in electrical and electronics engineering from Jawaharlal Nehru Technological University, Kakinada, India, in 2013, and the M.Tech. degree in industrial power and automation from the National Institute of Technology Calicut, India, in 2016, where he is currently pursuing the Ph.D. degree in electrical engineering. His main research interests include dc–dc converters and renewable energy integration.

KUMARAVEL SUNDARAMOORTHY (M'09–SM'16) was born in Tanjaore, India, in 1981. He received the B.E. degree in E.E.E from Bharathidasan University, Thiruchirappalli, India, the M.Tech. degree in power systems from the National Institute of Technology Thiruchirappalli, and the Ph.D. in electrical engineering from the National Institute of Technology Calicut, India. He completed the Post-Doctoral Fellowship in power systems with the University College Dublin, Ireland.
He has been an Assistant Professor with the Department of Electrical Engineering, National Institute of Technology Calicut, Kerala, since 2008. His major areas of research are distributed generation, applications of power converters in renewable energy sources, and artificial intelligence.

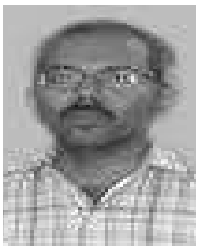

ASHOK SANKAR (M'94–SM'05) was born in Kottayam, India. He received the B.Sc. degree in E.E.E from the Regional Engineering College, Calicut, India, the M.Tech. degree in energy from IIT Delhi, and the Ph.D. degree from IIT Bombay. He is currently a Professor and the Head of the Department of Electrical Engineering, National Institute of Technology Calicut. His major areas of research are distributed generation, microgrid, deregulation and power quality.